JPL Publication 16-2

Mars Exploration Rover Spirit End of Mission Report

John L. Callas
Mars Exploration Rover Project
Jet Propulsion Laboratory

National Aeronautics and Space Administration

Jet Propulsion Laboratory
California Institute of Technology
Pasadena, California

December 2015

This research was carried out at the Jet Propulsion Laboratory, California Institute of Technology, under a contract with the National Aeronautics and Space Administration.

CONTENTS

END OF MISSION REPORT FOR THE MARS EXPLORATION ROVER SPIRIT

John L. Callas
Project Manager

ABSTRACT

The Mars Exploration Rover (MER) Spirit landed in Gusev crater on Mars on January 4, 2004, for a prime mission designed to last three months (90 sols). After more than six years operating on the surface of Mars, the last communication received from Spirit occurred on Sol 2210 (March 22, 2010). Following the loss of signal, the Mars Exploration Rover Project radiated over 1400 commands to Mars in an attempt to elicit a response from the rover. Attempts were made utilizing Deep Space Network X-Band and UHF relay via both Mars Odyssey and the Mars Reconnaissance Orbiter. Search and recovery efforts concluded on July 13, 2011. It is the MER project's assessment that Spirit succumbed to the extreme environmental conditions experienced during its fourth winter on Mars. Focusing on the time period from the end of the third Martian winter through the fourth winter and end of recovery activities, this report describes possible explanations for the loss of the vehicle and the extent of recovery efforts that were performed. It offers lessons learned and provides an overall mission summary.

1 SCIENCE HIGHLIGHTS

Spirit's six-year exploration of Mars produced an enormous number and range of scientific discoveries and insights [1, 2, 3]. Two discoveries stand out as the most important scientific contributions of Spirit: the identification of widespread water-related soil deposits just below the surface [4, 5], and identifying of carbonate minerals in the Comanche outcrop [6]. Early in the mission, verifying the presence of goethite in the Columbia Hills—a hydrated iron oxide mineral that only forms in the presence of liquid water—confirmed the former presence of water at Spirit's landing site, fulfilling one of the prime science objectives of the mission.

Spirit's contributions to Mars science did not stop there. Dynamic observations of dust devils, clouds, and other atmospheric phenomena added to our understanding of Mars meteorology. In addition, the mechanical properties of various soils were investigated, leading to the identification of several iron meteorites. Three distinct volcanic regimes were identified and characterized (unaltered Hesperian basalt flows in the Gusev Plains, a wide variety of basaltic alteration products in the older Columbia Hills, and a more alkalic, volcaniclastic assemblage around Home Plate in the Inner Basin). The presence of substantial unaltered olivine in the plains rocks provided evidence that the basaltic plains probably have experienced only a cold and arid climate since their formation. In contrast, a diverse suite of rocks with more extensive chemical alteration in the West Spur and Husband Hill bedrock indicates that aqueous processes were more pervasive during the earliest epochs in this region. Because the Columbia Hills may be representative of typical ancient cratered terrain on Mars, this investigation may be applicable to geologic study of much of the planet. And the volcaniclastic formations associated with Home Plate indicate a completely distinct volcanic style from that responsible for the Columbia Hills.

Spirit found widespread multiple occurrences of a layer of sulfur-rich salts (ferric sulfate, calcium salts) and hydrated amorphous silica millimeters beneath the surface of the soil. The most likely explanations for the presence of these minerals are all processes related to mobilization by liquid water or steam. The evidence for such water-related processes in a surficial soil layer implies much more recent hydrous activity than that responsible for the ancient bedrock of Husband Hill. Analysis of these sulfate salts shows a chemical connection with the surrounding rocks in each case, providing additional evidence for an origin related to hydrothermal activity or acidic volcanic vapors. Furthermore, a strong 6-micron water band seen by Mini-TES in the Tyrone ferric salt deposit indicates that the salts are substantially hydrated. This suggests that hydrated sulfates may be an important reservoir for near-surface water at low latitudes over much of Mars, and could be responsible for the low-latitude hydrogen observed in Mars Odyssey gamma-ray and neutron data.

The discovery of high-purity opaline silica deposits by Spirit (see Figure 1.1) is particularly significant because the hydrothermal conditions that they imply could have led to locally habitable conditions. Any process that involves re-precipitation of silica from fluids can also provide a mechanism for preserving evidence of microbes; indeed, morphologic microfossils are well preserved in some terrestrial siliceous sinter deposits. These types of materials could be excellent candidates for future sample return missions. And finally, in Scamander crater, Spirit was able to establish that the sulfate-rich sands in which the rover was embedded have a vertical gradient in their chemistry (see Figure 1.2). This gradient is consistent with vertical modification by downward migration of soluble salts, enriching the upper section in calcium sulfates and

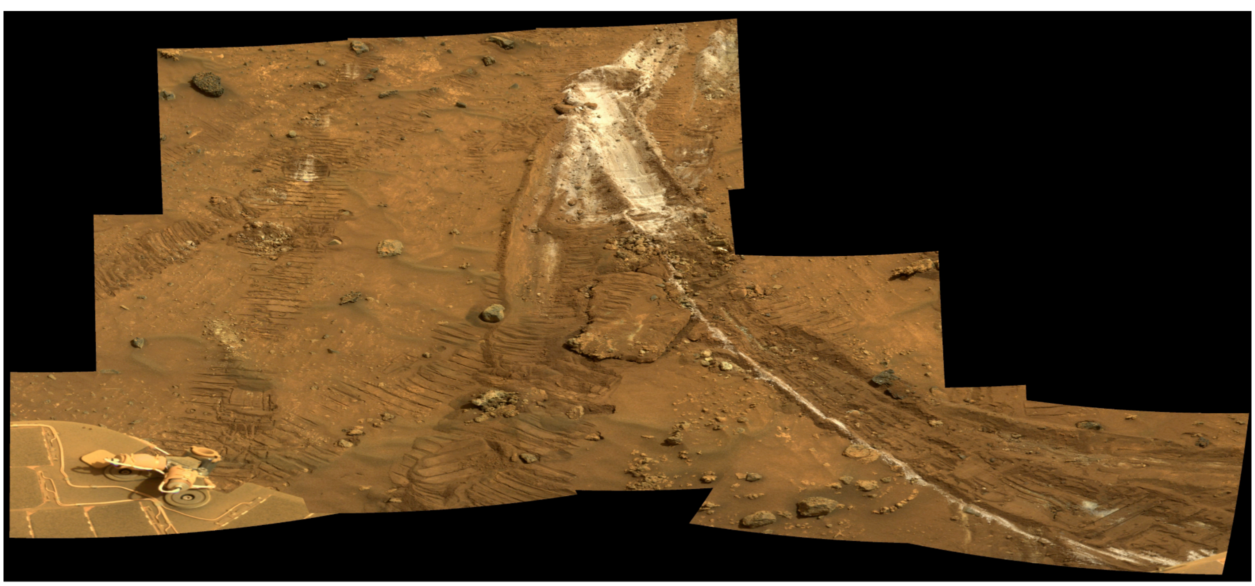

Figure 1.1 *Color Pancam image from Sol 1202 of the disturbed soil, named "Gertrude Weise."*

silica. Downward migration is likely a consequence of thin films of water associated with solid-state greenhouse-induced warming of snow packs during periods of high obliquity.

Figure 1.2 *Color Pancam image from Sol 2163 of the disturbed soil around Spirit at the location named "Troy."*

Figure 1.3 *Color Pancam image from Sol 689 of the "Comanche" outcrop.*

A detailed and painstaking joint analysis of Mössbauer, APXS, and Mini-TES data acquired on the Comanche outcrop near the top of Husband Hill (see Figure 1.3) revealed the presence of significant amounts of iron and magnesium carbonate minerals in these rocks. Previously, carbonates were found in ALH-84001 and CRISM spectra of Nili Fossae, but this is the first positive identification of this important mineral in its geologic context. The apparently similar chemical compositions of Comanche, ALH 84001, and Nili Fossae carbonates suggest a common formation pathway, with multiple lines of evidence pointing to aqueous processes under hydrothermal conditions. The Comanche outcrops and their substantial carbonate concentration (16 to 34 wt %) imply extensive aqueous activity under near-neutral pH conditions that would be conducive to habitable environments on early Mars. The well separated Nili Fossae and Gusev crater carbonate locations (~6300 km on a great circle) imply that such environments have multiple occurrences in Noachian terrain. The high carbonate concentration in the Comanche outcrops is evidence for CO_2 greenhouse-type conditions on a wet and warm early Mars, and the subsequent sequestering of at least part of that atmosphere in carbonate minerals.

The discovery of carbonate in Comanche was not confirmed until four years after measurements were obtained on the outcrop; indeed, after Spirit had ceased communicating with the Earth. The circumstances of this discovery illustrate what may be the most important scientific legacy of Spirit: the immense, rich data set left behind for future research.

References

1. Arvidson, R. E., S. W. Squyres, R. C. Anderson, J. F. Bell, III, D. Blaney, J. Brückner, N. A. Cabrol, W. M. Calvin, M. H. Carr, P. R. Christensen, B. C. Clark, L. Crumpler, D. J. Des Marais, P. A. de Souza, Jr., C. d'Uston, T. Economou, J. Farmer, W. H. Farrand, W. Folkner, M. P. Golombek, S. Gorevan, J. A. Grant, R. Greeley, J. Grotzinger, E. Guinness, B. C. Hahn, L. Haskin, K. E. Herkenhoff, J. A Hurowitz, S. Hviid, J. R. Johnson, G. Klingelhöfer, A. H. Knoll, G. Landis, C. Leff, M. Lemmon, R. Li, M. B. Madsen, M. C. Malin, S. M. McLennan, H. Y. McSween, D. W. Ming, J. Moersch, R. V. Morris, T. Parker, J. W. Rice, Jr., L Richter, R. Rieder, D. S. Rodionov, C. Schröder, M. Sims, M. Smith, P. Smith, L. A. Soderblom, R. Sullivan, S. D. Thompson, N. J. Tosca, A. Wang, H. Wänke, J. Ward, T. Wdowiak, M. Wolff, A.Yen, 2006, Overview of the Spirit Mars Exploration

Rover Mission to Gusev Crater: Landing site to Backstay Rock in the Columbia Hills, *J. Geophys. Res.*, 111, E2, E02S01 doi: 10.1029/2005JE002499.

2. Arvidson, R.E., S. Ruff, R.V. Morris, D.W. Ming, L. Crumpler, A. Yen, S.W. Squyres, R.J. Sullivan, J.F. Bell III, N.A. Cabrol, B.C. Clark, W. Farrand, R. Gellert, R. Greenberger, J.A. Grant, E.A. Guinness, K.E. Herkenhoff1, J. Hurowitz , J.R. Johnson, G. Klingelhöfer, K. Lewis, R. Li, T. McCoy, J. Moersch, H.Y. McSween, S. Murchie, M. Schmidt, C. Schröder, A. Wang, S. Wiseman, M.B. Madsen, W. Goetz, S. McLennan, 2008, Spirit Mars Rover Mission to the Columbia Hills, Gusev Crater: Mission Overview and Selected Results from the Cumberland Ridge to Home Plate, *J. Geophys. Res*., 113, E12S33, doi: 10.1029/2008JE003183.
3. Arvidson, R. E., J.F. Bell III, P. Bellutta, N.A. Cabrol, J. G. Catalano, L. Crumpler, D. J. Des Marais, T. Estlin, W. Farrand, R. Gellert, J. A. Grant, R. Greenberger, E. A. Guinness, K. E. Herkenhoff, J. A. Herman, K. Iagnemma, J. R. Johnson, G. Klingelhöfer, R. Li, K. A. Lichtenberg, S. Maxwell, D. W. Ming, R.V. Morris, M. Rice, S. Ruff, A. Shaw, K. Siebach, P. de Souza, A. Stroupe, S. W. Squyres, R. J. Sullivan, K. Talley, J. Townsend, A. Wang, J. Wright, A. Yen, 2010, Spirit Mars Rover Mission: Overview and Selected Results from the Northern Home Plate Winter Haven to the Side of Scamander Crater, *J. Geophys. Res.,* 115, E00F03, doi:10.1029/2010JE003633.
4. Squyres, S. W., R. Arvidson, S. Ruff, R. Gellert, R. Morris, D. Ming, L. Crumpler, J. Farmer, D. Des Marais, A. Yen, S. McLennan, W. Calvin, B. Clark, A. Wang, 2008, Detection of Silica-Rich Deposits on Mars, *Science,* 320, 1063 doi: 10.1126/science.1155429.
5. Ruff, S. W., J. D. Farmer, W. M. Calvin, K. E. Herkenhoff, J. R. Johnson, R. V. Morris, M. S. Rice, R. E. Arvidson, J. F. Bell III, P. R. Christensen, and S. W. Squyres, 2011, Characteristics, distribution, origin, and significance of opaline silica observed by the Spirit rover in Gusev crater, Mars, *J. Geophys. Res*., 116, E00F23, doi:10.1029/2010JE003767.
6. Morris, R. V., S. W. Ruff, R. Gellert, D. W. Ming, R. E. Arvidson, B. C. Clark, D. C. Golden, K. Siebach, G. Klingelhöfer, C. Schröder, I. Fleischer, A. S. Yen, S. W. Squyres, 2010, Identification of Carbonate-Rich Outcrops on Mars by the Spirit Rover, *Science,* doi: 10.1126/science.1189667.

2 ENVIRONMENTAL CHALLENGES

The Mars Exploration Rovers, Spirit and Opportunity, are solar-powered surface-roving vehicles (see Figure 2.1). Spirit was located at approximately 14° S latitude and Opportunity was located at about 2° S latitude. The prime mission for the rovers was 90 sols (Martian days). With no consumable on board, mission duration was greatly influenced by the reduction in available energy as air-fall dust accumulated on the solar arrays and Mars advanced into the light-limited winter season. Although designed with a high likelihood of operation for 90 sols, the long-term expectation was that the rovers would lose capability due to excess dust obscuring the solar arrays and the reduced winter light generating insufficient energy to survive the cold temperatures of the southern hemisphere winter.

At the beginning of the mission (Sol 1), for example, Spirit generated more than 900 watt-hours of energy each sol. By Sol 90 (end of the prime mission), the daily energy production had dropped to about 600 watt-hours. In spite of this, operations continued and the mission was extended for both rovers.

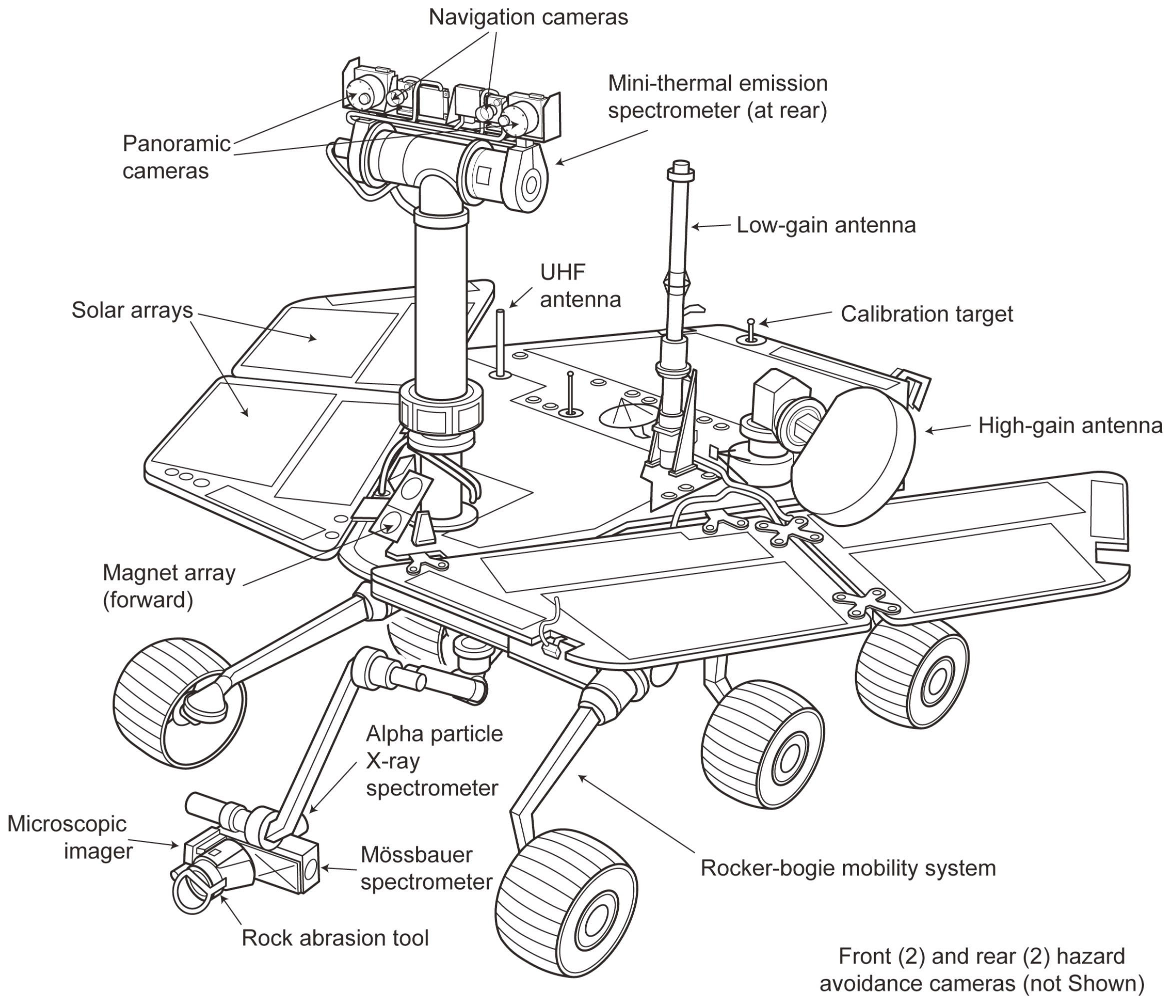

Figure 2.1 *Diagram of the Mars Exploration Rover.*

By the time of the first winter (Sol-A 254), the solar arrays were at only about 70% performance for Spirit due to dust obscuring 30% of the arrays, lowering daily energy production to about 400 watt-hours. (The project uses a term called dust factor. A dust factor of 1 is a perfectly clean solar array, 0 is a completely obscured array, 0.5 means 50% of the solar array is covered by dust, etc.) Figure 2.2 shows Spirit’s solar array dust factor over the entire mission. Around Sol 420, Spirit experienced her first solar array dust cleaning event. These cleanings were likely wind-related (e.g., gusts or dust devils) and effectively blew large amounts of dust off the rover’s solar arrays. They occurred unpredictably, but with some seasonality and with varying effectiveness. After the first instance of dust removal, energy production increased from around 400 watt-hours per sol to over 700 watt-hours, a significant improvement. This episodic pattern of array cleaning was a principal contributor to the longevity of both rovers and their multiple winter survivals. Cleaning events seemed to preferentially occur when Spirit was exposed to the wind at topographically high locations, such as ridge crests and summits.

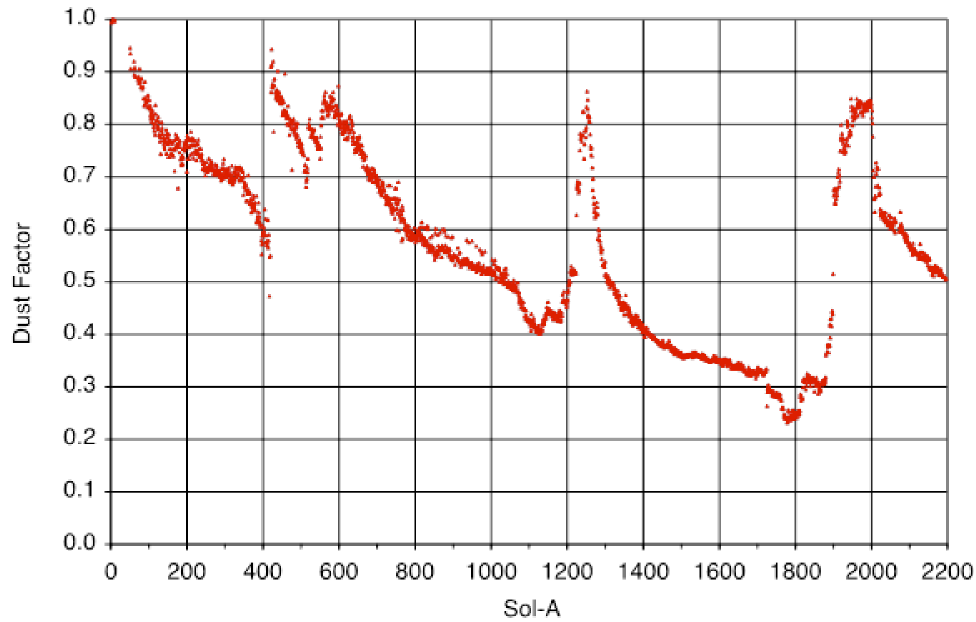

Figure 2.2 *Spirit's historical dust factor over the entire mission.*

3 Loss of Mobility

On Sol 779, after operating for more than two Earth years, the right-front drive wheel actuator on Spirit failed. Because of the design of the motor, which utilized magnetic detents and a large-reduction (1500:1) gearbox, a failed wheel will not freely spin. Spirit's wheel would remain locked, greatly compromising further mobility. Figure 3.1 shows the Sol 781 front Hazard Avoidance Camera (Hazcam) image capturing the effects of the failed wheel on the local terrain. No explanation has been established for the wheel failure, although a motor brush failure is one possibility. Also, the actuators were operational well past their design life. Spirit had driven over 6.5 kilometers at the time of the wheel failure, greatly exceeding the design requirement of only 1 kilometer for the rover mobility system.

Although with compromised mobility, Spirit was able to conduct a successful science and exploration campaign. Indeed, the trenching action of the locked wheel was largely responsible for the initial discovery of opaline silica mentioned above. Figure 3.2 shows Spirit's odometry history over the entire mission. The change in progress is apparent after the Sol 779 right-front wheel failure.

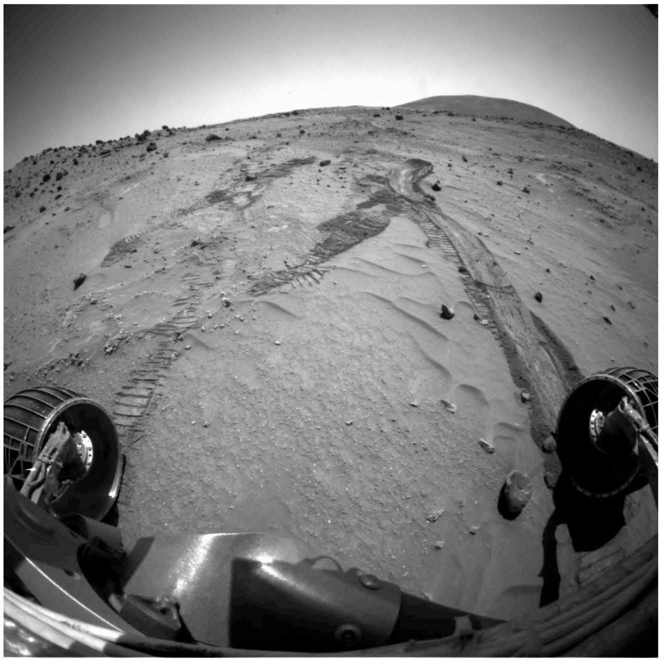

Figure 3.1 *Sol 781 front Hazcam image.*

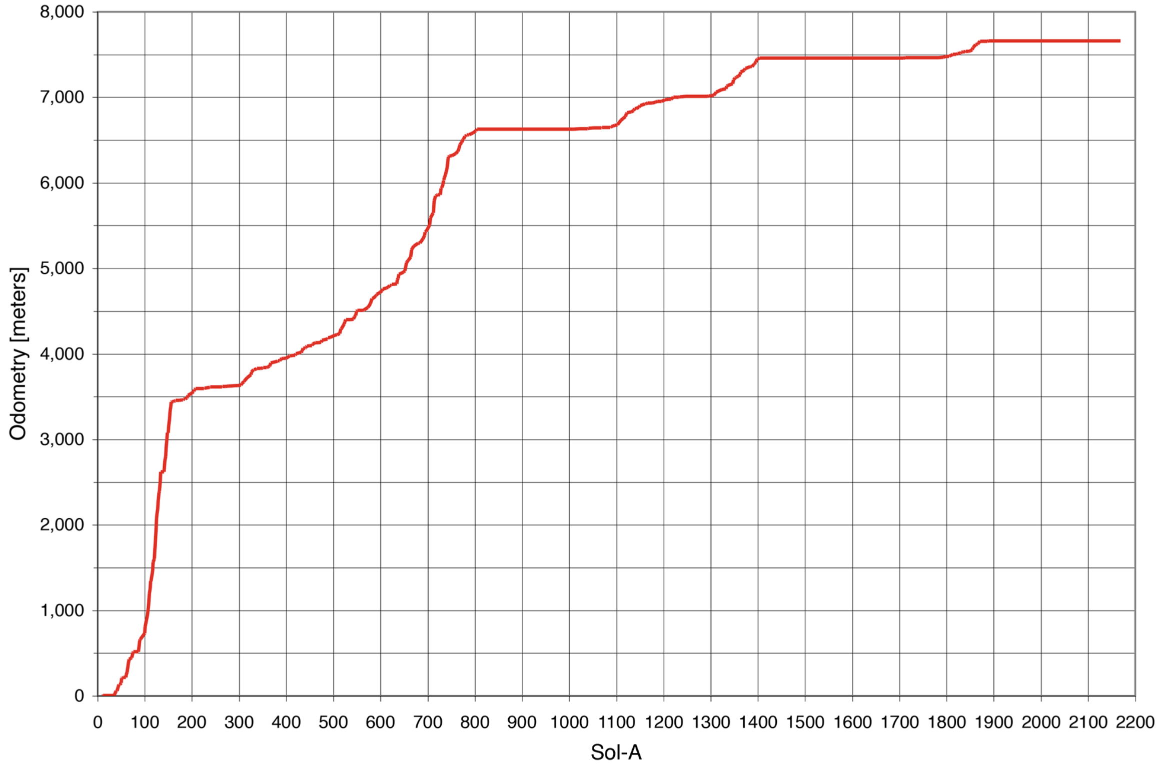

Figure 3.2 *Spirit's odometry history.*

4 Winter Strategies

Active measures taken by the operations team also contributed to each rover's longevity. For Spirit, Gusev crater was a dustier environment then Meridiani was for Opportunity, and it was also further south, making the winters longer and darker. The operations team positioned Spirit each winter with a northerly tilt to enhance the solar insolation on the solar arrays (see Table 4.1). During her first winter, Spirit was located on the north facing slopes of Husband Hill. Here the terrain afforded the rover slopes around 13° to 14° of northerly tilt. With a healthy dust factor and favorable terrain, Spirit was able to remain active throughout her first winter.

Because of an ever-decreasing dust factor (see Table 2.1), each successive winter became a more difficult survival challenge. After the first winter, the rover was required to be stationary

Table 4.1 Summary of Spirit's winter tilt, dust factor, and daily energy production

Winter	Sol-A	N. Tilt	Dust Factor	Energy Production
1	254	13.5°	0.71	434 watt-hours
2	923	11.5°	0.53	278 watt-hours
3	1591	28.8°	0.35	227 watt-hours
4	2260	−9.2°	<0.50	<133 watt-hours

(Dust factor and energy production for Winter 4 are not known due to loss of contact.)

for the season to conserve energy. More significantly, each subsequent winter necessitated positioning the rover, now with limited mobility, on an increasingly northerly tilt. Figure 4.1 shows a reconstruction of Spirit's position for each of the four Martian winters.

With each passing sol, the available solar array energy was reduced. Figure 4.2 provides the historical energy production based on the Martian year (Sub-solar longitude). Southern winter occurs at a sub-solar longitude (Ls) of 90°. Year 1 is the period from landing (Sol 1) to the first Martian fall. The first winter occurs in Year 2. The fourth winter occurs in Year 5. Note the precipitously lower energy production in the approach to the last winter, the result of a lower dust factor combined with unfavorable tilt.

The Sol 779 wheel failure limited the amount of slope Spirit could climb to achieve improved solar insolation to about 12°. Spirit remained stationary on a modest slope (11.5°) during her second winter. With net increasing amounts of dust on the arrays, the third winter required an even steeper northerly slope for survivability, but the failed wheel would prevent Spirit from climbing those steeper slopes. The project was fortunate to have Spirit at Home Plate. Here the rover was driven from the top of Home Plate down the side slope. This afforded the rover a near 30° northerly tilt. Spirit could not have achieved that slope by driving up.

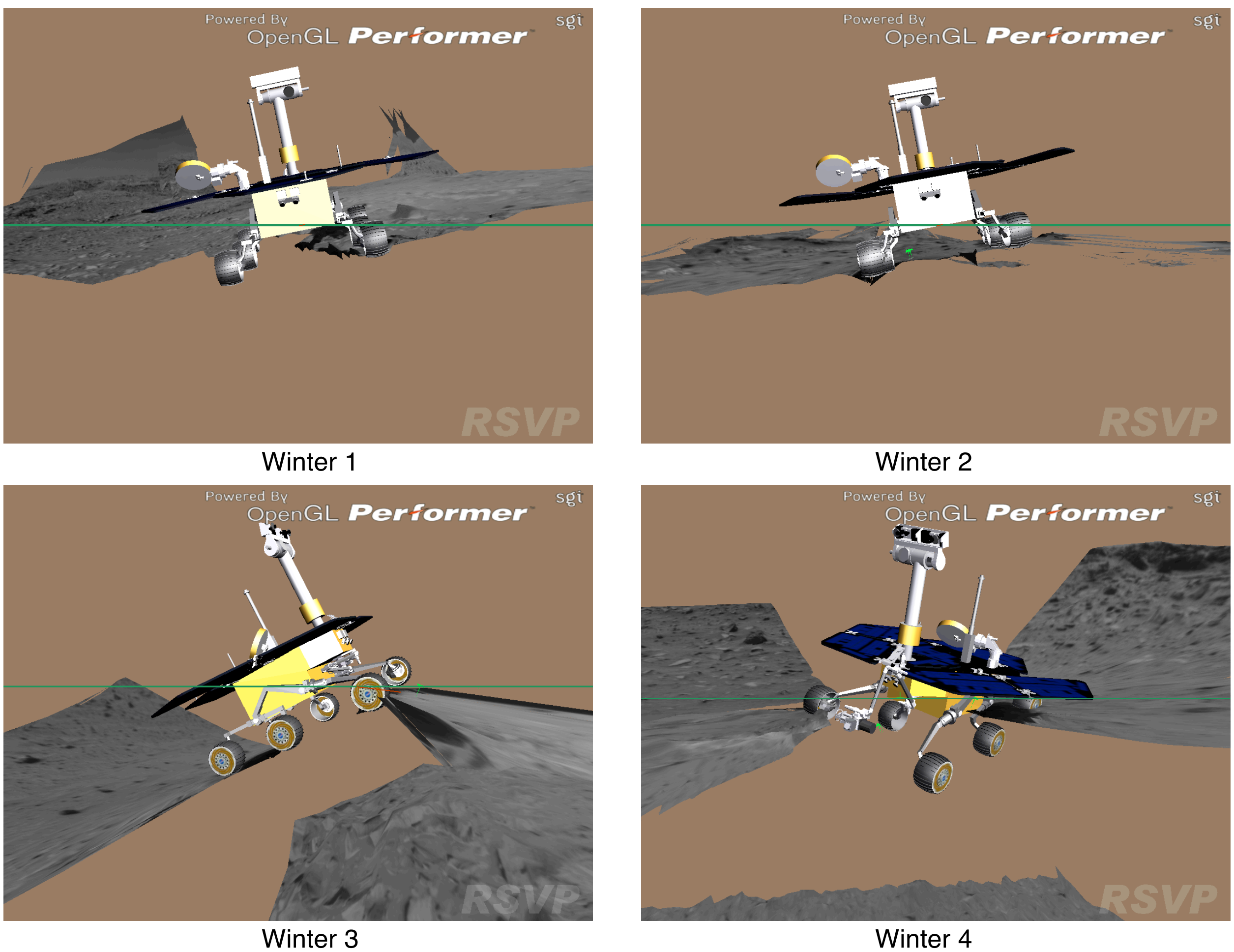

Figure 4.1 *Spirit's winter positions. All simulated views are local level, looking due east with north off to the left.*

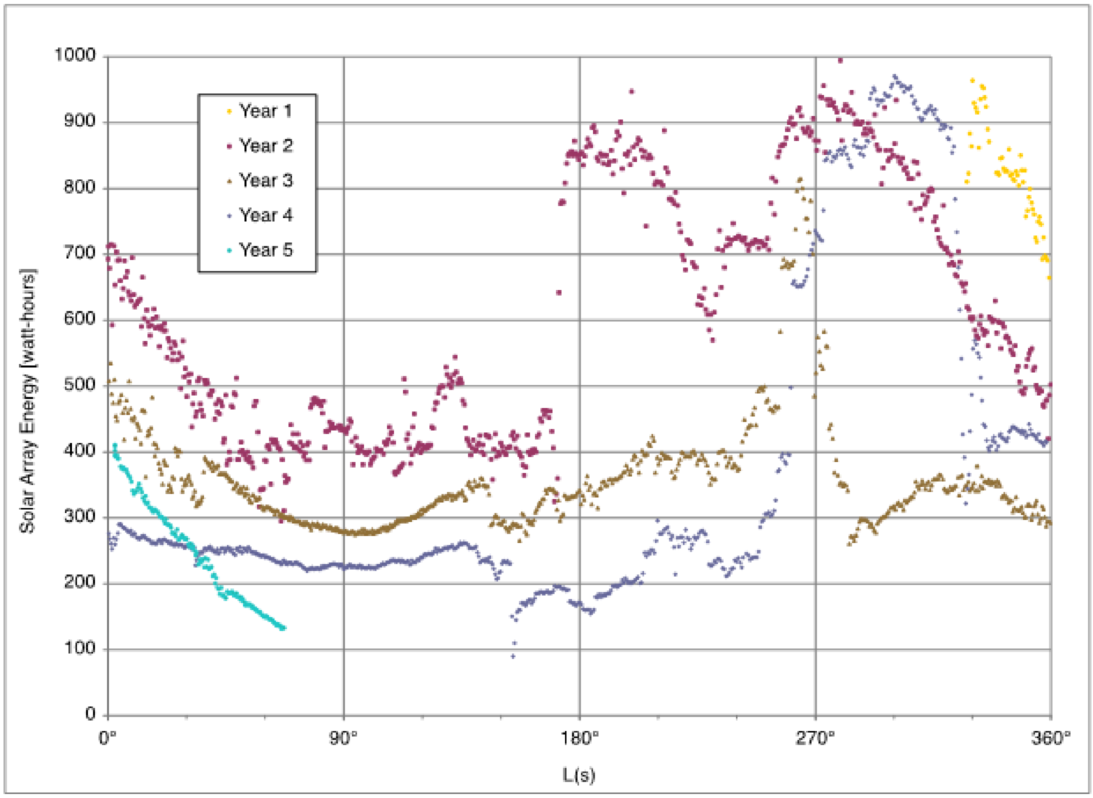

Figure 4.2 *Spirit's daily energy production for each Martian year.*

5 FOURTH WINTER SCIENCE PLAN

At the conclusion of the third winter, the project was left with the dilemma of where to position Spirit for the fourth winter. Realizing the downward secular trend in solar array dust factor, even with occasional dust cleaning events, Spirit would require even steeper slopes than previous winters. A detailed survey of the terrain showed no terrain features where the rover could achieve the necessary steep slopes. Even if they existed, the rover could not access them by driving up, only by driving down from above.

The project made the decision to use the time before the next winter to conduct science in new terrains to the south. Orbital imagery revealed two features of interest, named Goddard and von Braun, about 150 meters away (see Figure 5.1). In addition to new science, these features (especially Goddard) presented possible opportunities for the rover to climb their interiors and achieve some amount of northerly tilt. Goddard exhibits a ring of light-toned material just inside its crater. Reaching that material was considered an important science objective while providing an opportunity to achieve a beneficial tilt, although likely wouldn't be as steep as the north end of Home Plate during Winter 3.

Several paths were considered to reach the targets to the south. Figure 5.2 shows the results of some of the route planning. Initially, Route 1 back onto Home Plate then across to the south was the preferred route. It traveled along the best-characterized terrain, at least initially. In addition, Route 1 was the shortest path south and had the most downstream options. Route 2 was a little longer and required an initial traverse over less characterized terrain. It too had many downstream path options. Route 3 was the longest route and traveled over the least characterized terrain. Earlier observations suggested that the terrain along the west side of Home Plate may be problematic, with slopes and loose fines. The project prioritized the candidate paths with Route 1 being the first choice, Route 2 second, and Route 3, if both Routes 1 and 2 proved impassable, as the last option.

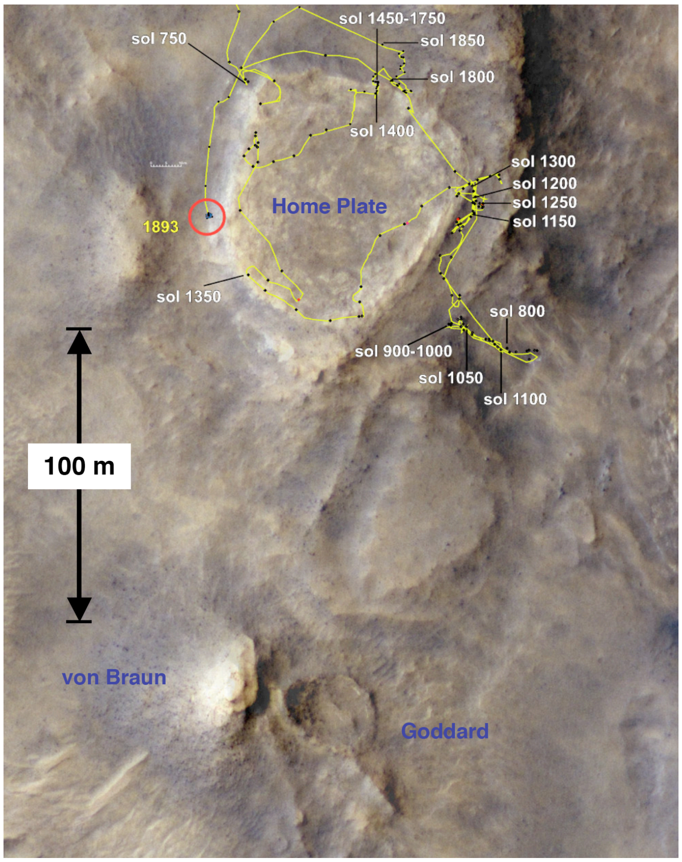

Figure 5.1 *Region south of Home Plate*

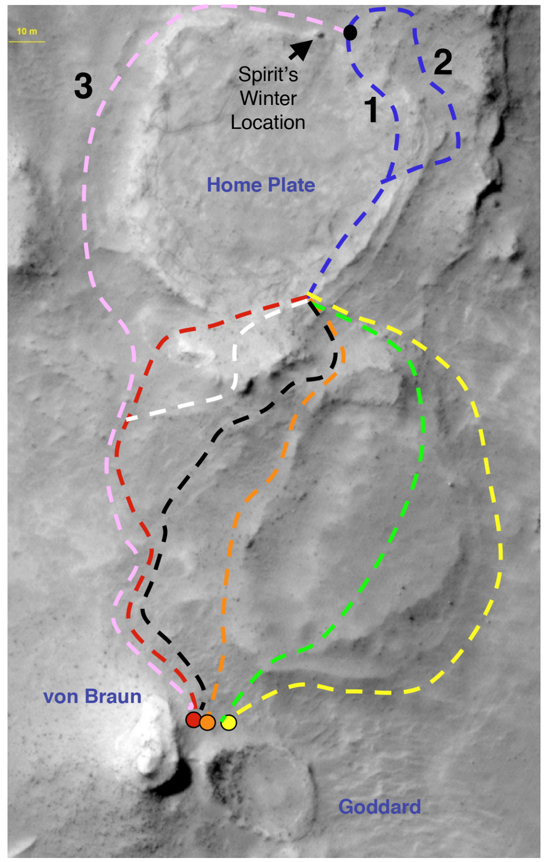

Figure 5.2 *Candidate routes to the south*

6 Rover Embeddings

After Sol 1800, Spirit began the move along Route 1, the traverse up onto Home Plate. Soon the rover began to experience difficulty negotiating terrain with moderate slopes. Figure 6.1 shows the Sol 1818 Hazcam images of the embedding that was occurring. After making extensive efforts, the project abandoned Route 1 on Sol 1829 and made the decision to pursue Route 2.

As a result of the embedding difficulty along Route 1, the project developed and implemented the use of hazard avoidance maps. The maps combined terrain slope information with science team assessments of soil types and terrain morphology to produce a red-yellow-green tabular 'map' of terrain hazards. This information was used tactically to make decisions about the safety of driving routes. Figure 6.2 illustrates the hazard map information.

Figure 6.1 *Sol 1818 Hazcam images showing the embedding of the rover wheels.*

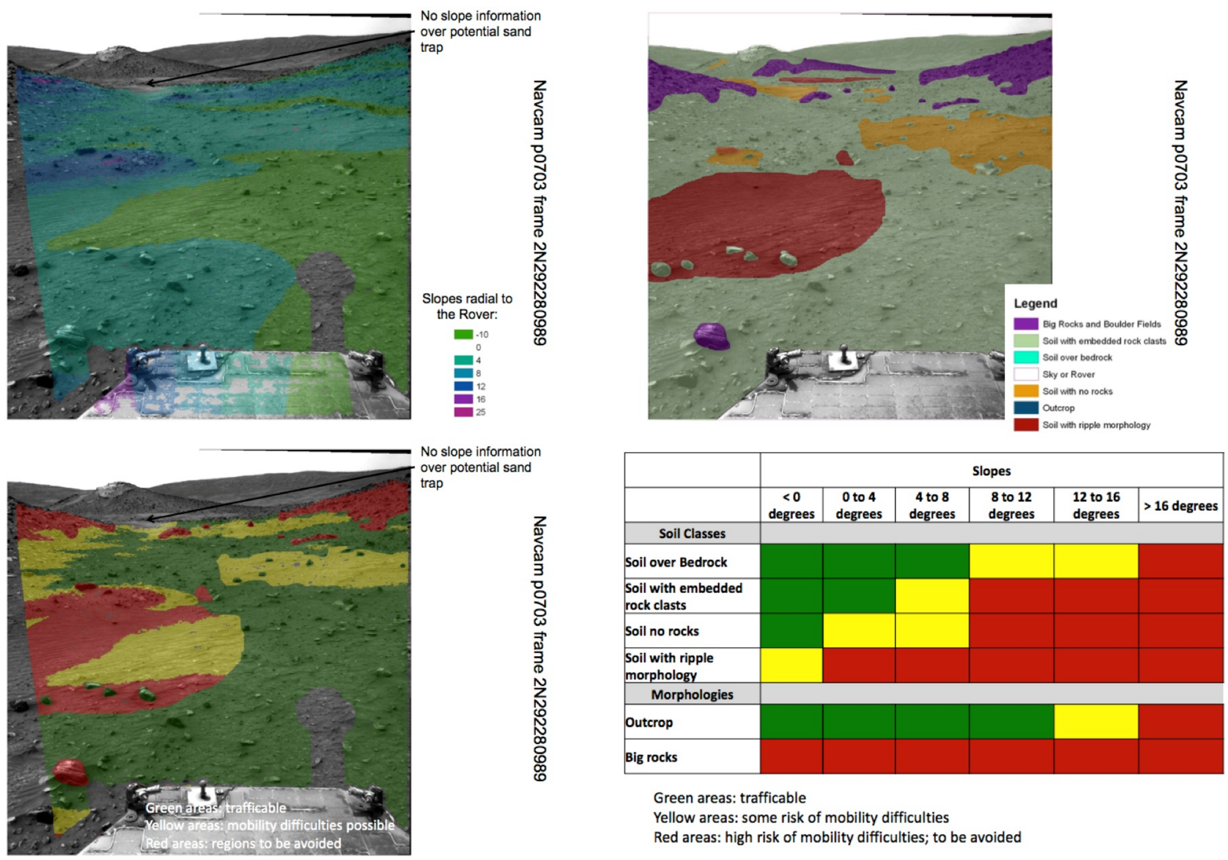

	Slopes					
	< 0 degrees	0 to 4 degrees	4 to 8 degrees	8 to 12 degrees	12 to 16 degrees	> 16 degrees
Soil Classes						
Soil over Bedrock	Green	Green	Green	Yellow	Yellow	Red
Soil with embedded rock clasts	Green	Green	Yellow	Red	Red	Red
Soil no rocks	Green	Yellow	Yellow	Red	Red	Red
Soil with ripple morphology	Yellow	Red	Red	Red	Red	Red
Morphologies						
Outcrop	Green	Green	Green	Green	Yellow	Red
Big rocks	Red	Red	Red	Red	Red	Red

Green areas: trafficable
Yellow areas: some risk of mobility difficulties
Red areas: high risk of mobility difficulties; to be avoided

Figure 6.2 *An example of hazard maps implemented after the Sol 1818 embeddings.*

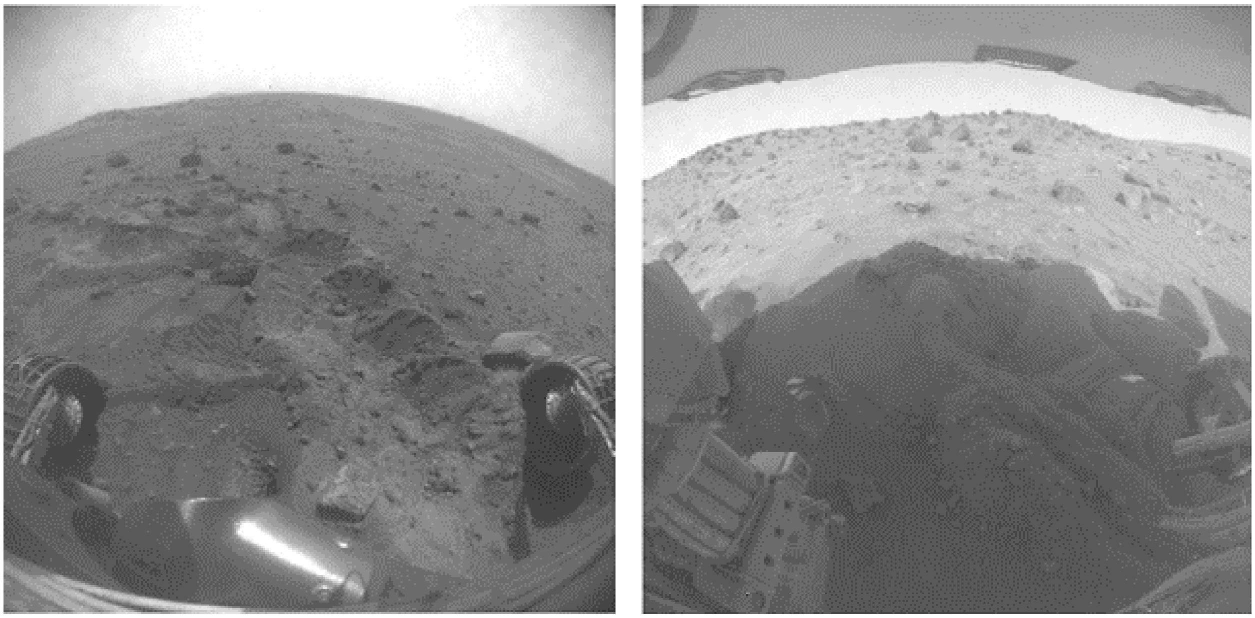

Figure 6.3 *Sol 1845 Hazcam images showing the embedding of the rover wheels.*

Before long, the Route 2 path around to the northeast of Home Plate also proved impassible. The rover again experienced wheel embedding while trying to mount modest slopes in loose terrain. Figure 6.3 shows the Sol 1845 Hazcam images of wheel embedding.

After several attempts to drive around Home Plate to the northeast, the embedding and problematic driving forced the project to abandon Route 2. This occurred on Sol 1843, fourteen sols after abandoning Route 1 and 49 sols since the departure from the rover's third winter haven. With the unsuccessful attempts along Routes 1 and 2, it is important to note that precious time had now elapsed to get Spirit south in time to conduct a science campaign in and around Goddard and von Braun and then get prepared for the coming winter.

Exercising their last option, the project started guiding the rover on the path around the west side of Home Plate along Route 3. Figure 6.4 shows Spirit's traverse around Home Plate just prior to her eventual embedding along Route 3.

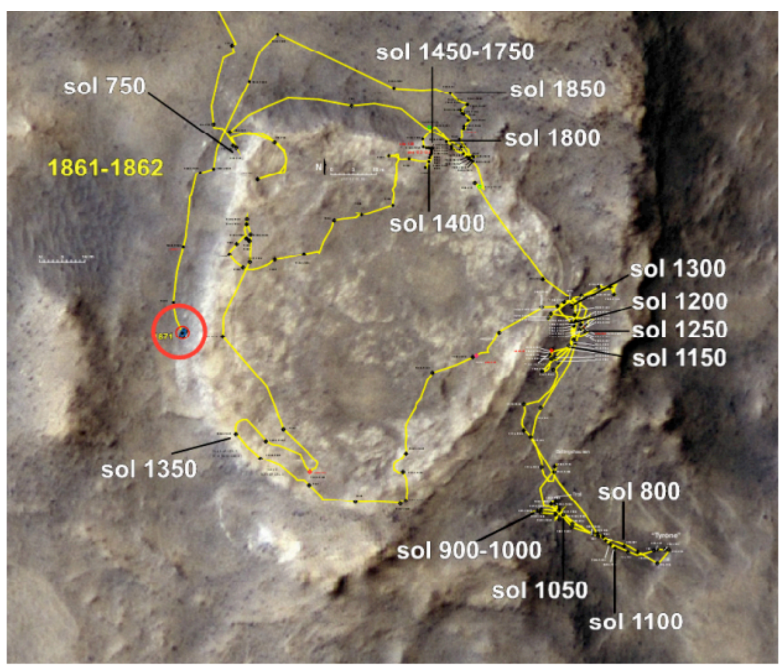

Figure 6.4 *Spirit's traverse around Home Plate by Sol 1871.*

Spirit initially made good westward progress along Route 3. Figure 6.5 is a Sol 1870 Navcam image showing an apparently hazard-free traverse path. But on Sol 1886, Spirit began to become embedded in a location on the west side of Home Plate, now called "Troy." Realizing the onset of embedding, the project, just as it had done for the embedding on Routes 1 and 2, made several tactical attempts to extricate the rover. But after several unsuccessful tries, on Sol 1899 a stall of the left middle wheel occurred. Upon investigation of the wheel stall and an assessment of the terrain, the project stood down from mobility operations. Figure 6.6 shows the Sol 1899 Hazcam images of the embedded rover wheels. Figure 6.7 summarizes the events leading up to and including the embedding at Troy.

Figure 6.5 *The Sol 1870 Navcam just prior to embedding at Troy. The embedding location is approximately dead-center of the image.*

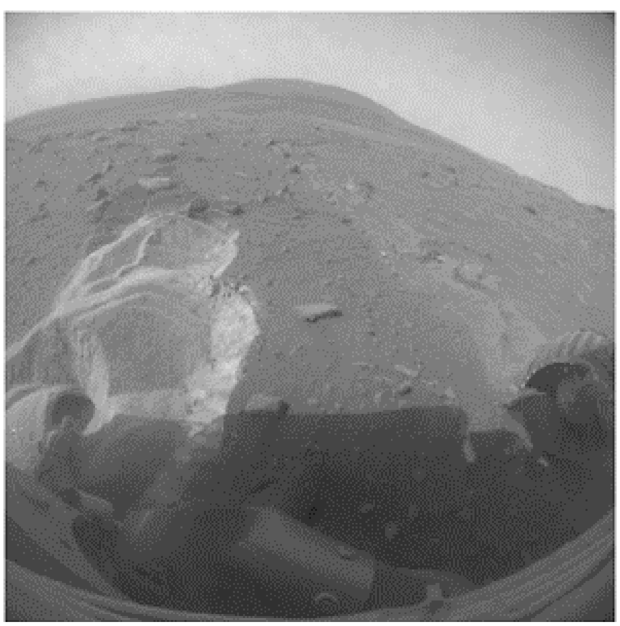

Sol 1899 Front Hazcam

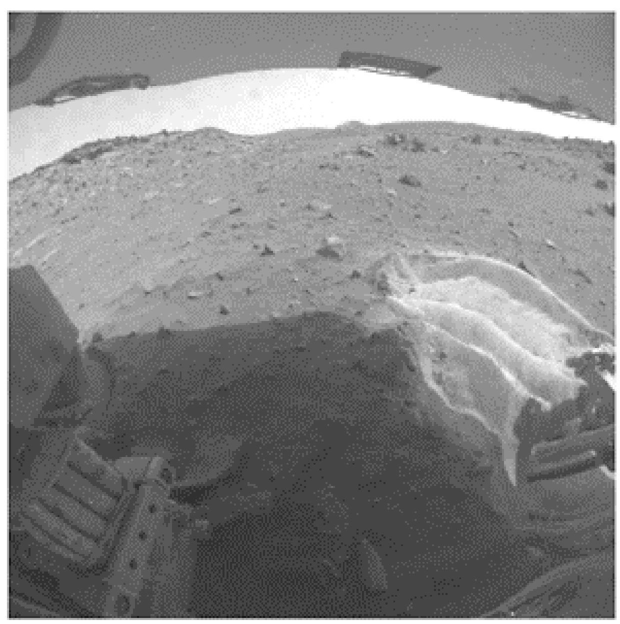

Sol 1899 Rear Hazcam

Figure 6.6 *Sol 1899 Front and Rear Hazcam images following the embedding at Troy.*

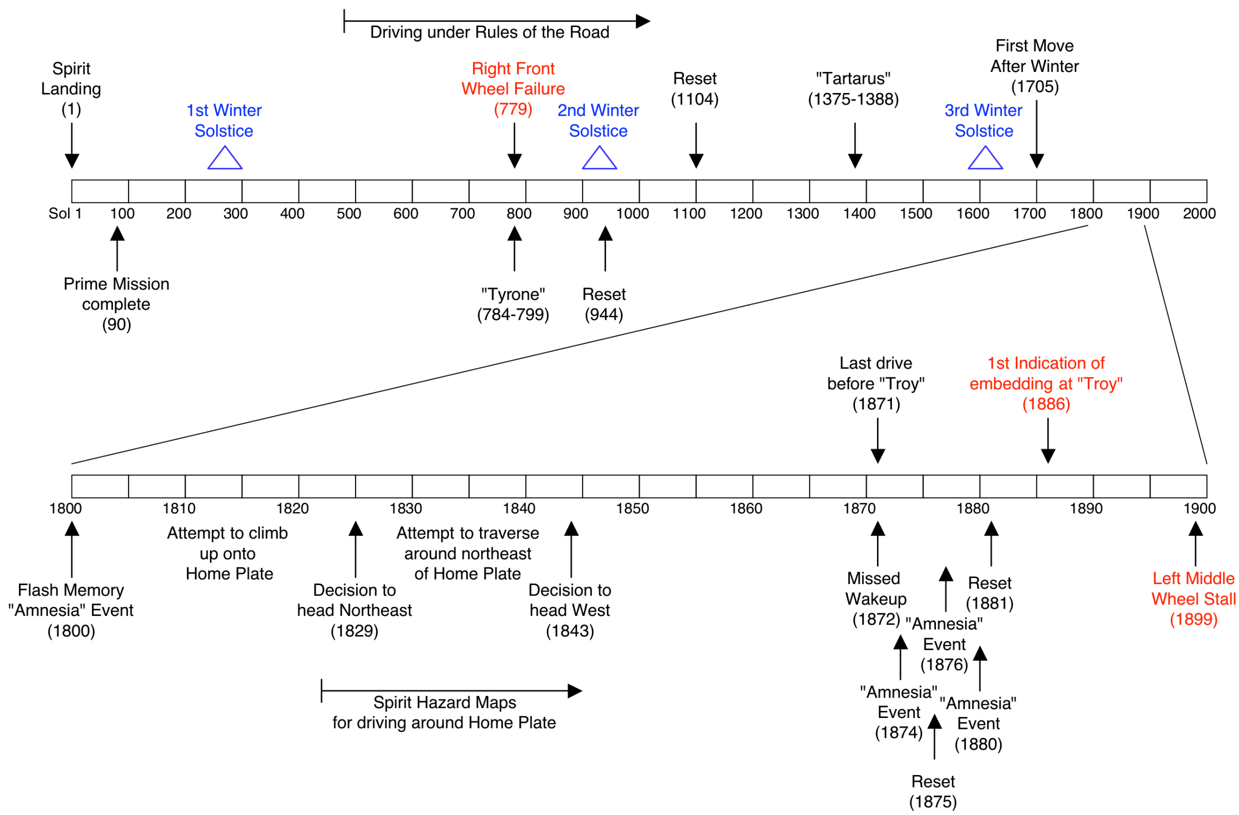

Figure 6.7 *Timeline of events leading up to Spirit's embedding at Troy.*

The proximate cause of the embedding is attributed to the rover breaking through an indurated crust into a hidden hazard of unconsolidated fines. The path south to the features Goddard and von Braun, which was dictated by the systematic exhaustion of all viable route options, led the rover to the unforseen hazard at Troy. This was a contributing cause. The root cause was that Spirit had degraded mobility (failed right-front wheel), which generated greater terrain shear forces that compromised the terrain's structural integrity, particularly on slopes. An undetected environmental hazard also existed along Spirit's inevitable route. Details of the embedding, including a root cause analysis, can be found in the JPL document "Report on the Spirit Embedding at Troy", dated June 17, 2010.

7 ROVER EXTRICATION EFFORT

Due to the embedding of Spirit at Troy, the project drew upon its experience with Opportunity's embedding at Purgatory. For the Purgatory embedding, the project recreated the embedding with the surface system testbed (SSTB) rover in the sandbox at JPL using custom soil simulants. Those tests provided guidance on procedures and expectations for the eventual successful extrication from Purgatory on Mars. The embedding of Spirit was significantly different, having just 5 operating wheels and its location in a more complex terrain environment. The situation prompted the MER project to pursue a more varied and ambitious ground-based simulation process, illustrated in Figures 7.1 and 7.2.

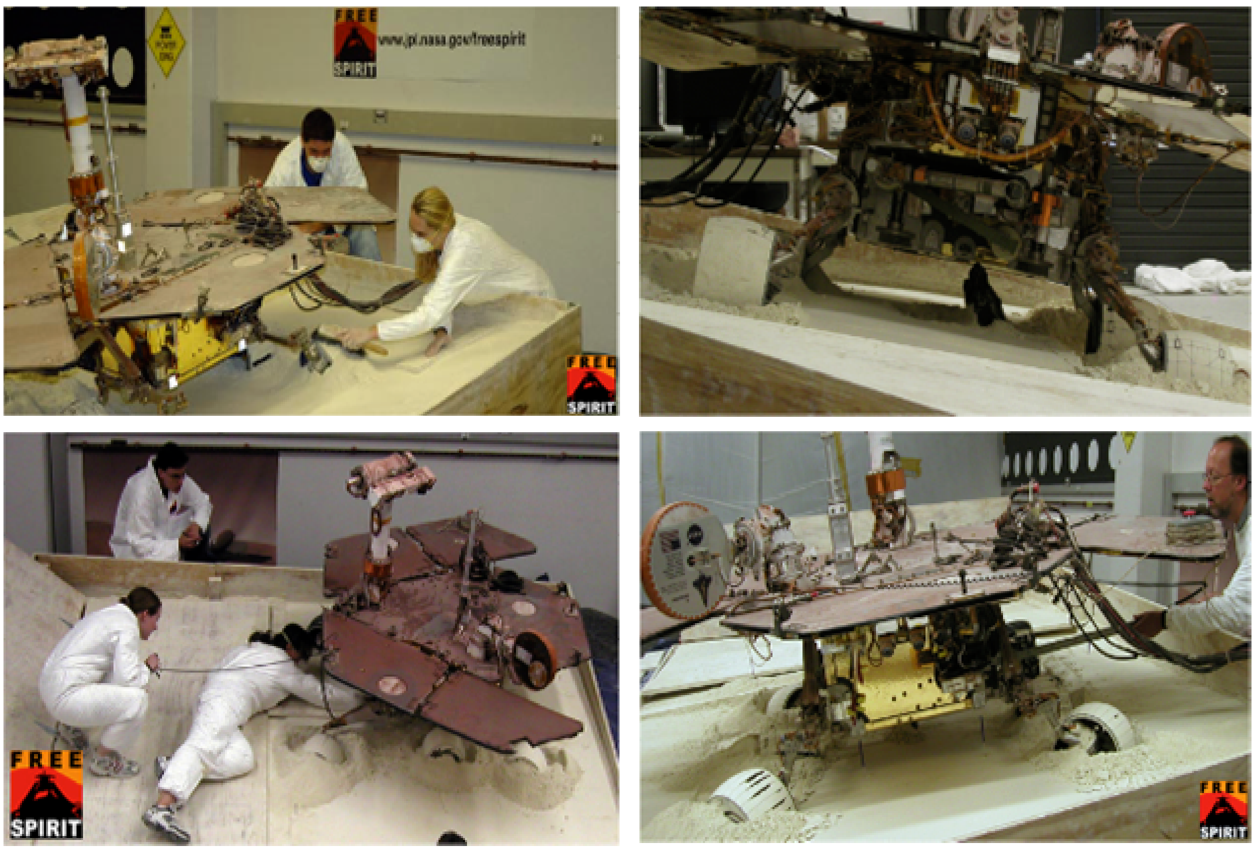

Figure 7.1 *Sandbox testing with the MER surface system testbed in simulated Mars conditions.*

After months of ground-based testing and independent project and programmatic reviews, extrication of Spirit was attempted on Mars. Table 7.1 summarizes the commanded motion of the rover since the commencement of extrication efforts on Sol 2078. On Sol 2092, the right rear wheel stalled. Subsequent investigation indicated that the wheel had failed, greatly reducing the likelihood of successfully extricating as a four-wheeled rover. However, important progress was achieved during the last nine extrication drives from Sol 2144 to 2162. Figure 7.3 shows the course plot and progress of those drives. Extrication had to be stopped due to the limited solar array energy anticipated during the advancing winter. The project needed to use the remaining time to prepare the rover for winter.

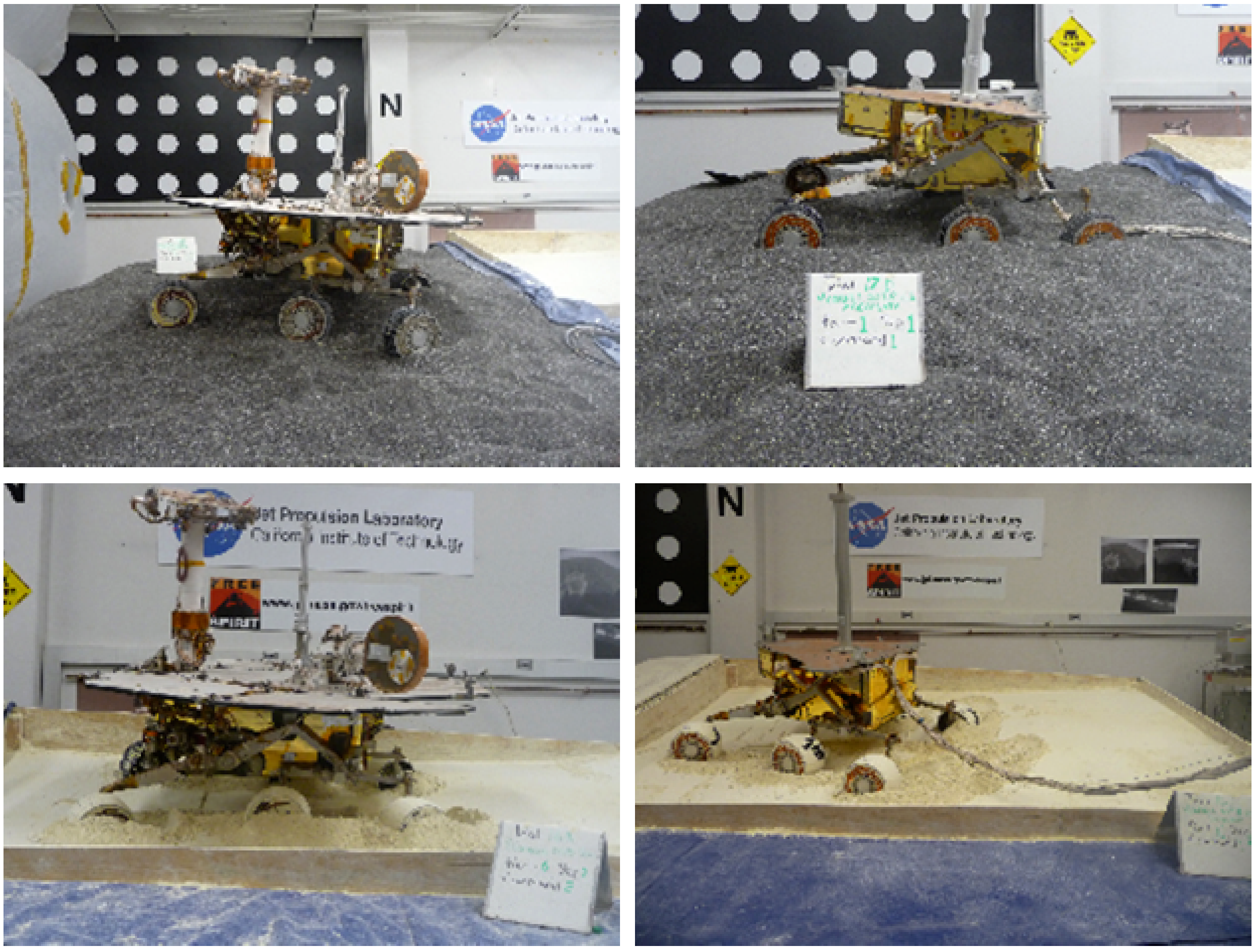

Figure 7.2 *Testing in simulant and aggregate of both the MER surface system testbed (SSTB) and the half-weight SSTB-Lite vehicle.*

Table 7.1 *Spirit's Extrication Drives*

Sol	Odometry [m]	Sol	Odometry [m]	Sol	Odometry [m]
2078	0.02	2120	0.02	2147	0.02
2088	0	2122	0.05	2150	0.05
2090	0.02	2126	0.02	2151	0
2092	0.02	2130	0.02	2152	0.04
2095	0.01	2132	0.01	2154	0.08
2099	0.01	2136	0.04	2156	0.01
2104	0	2138	0.02	2158	0.01
2109	0	2140	0.02	2161	0.03
2117	0.02	2143	0.01	2165	0.01
2118	0.01	2145	0.04	2169	0

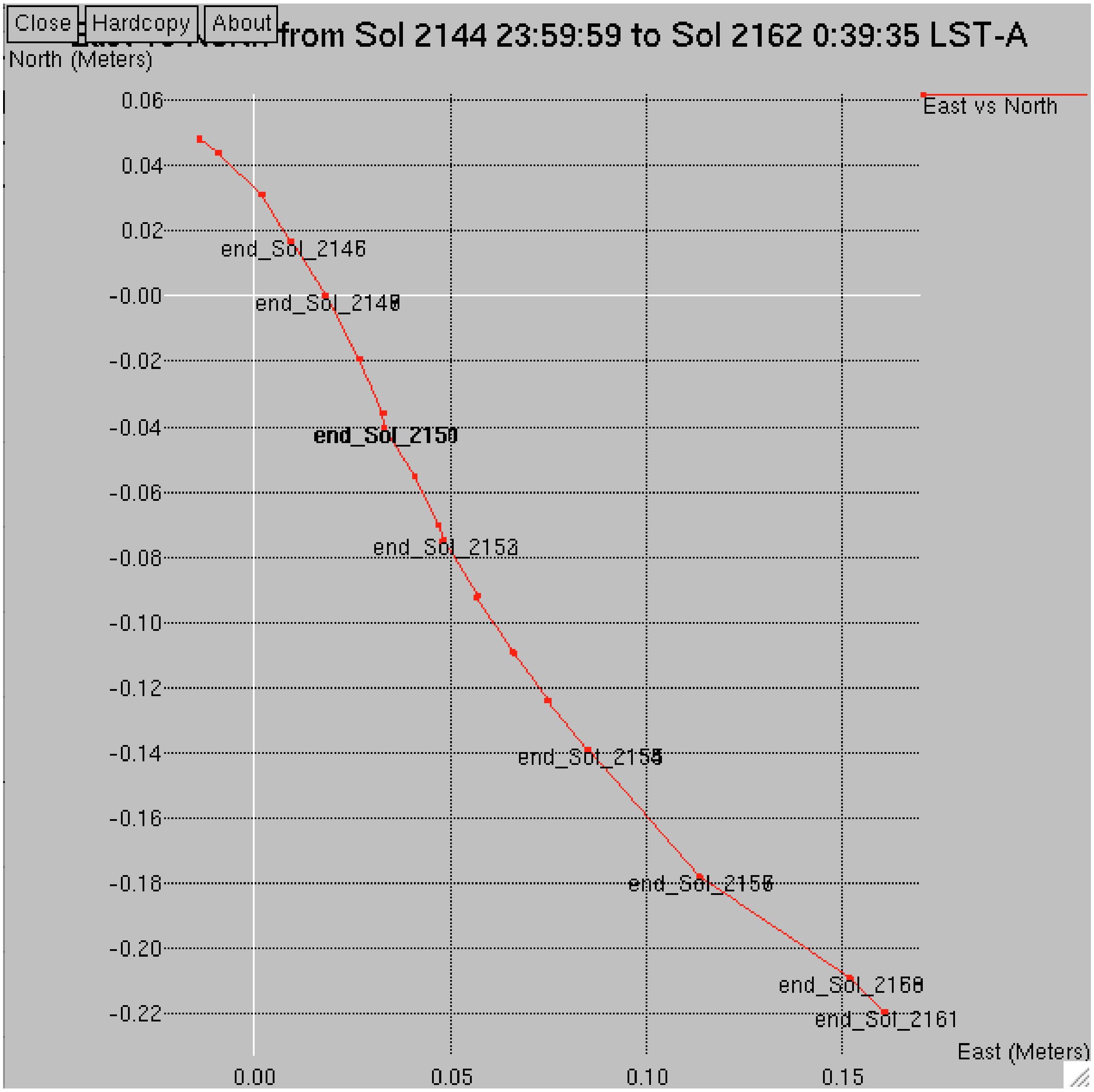

Figure 7.3 *Spirit's extrication progress from the last nine drive attempts.*

8 Preparations for the Fourth Winter

Without adequate time to extricate Spirit before the onset of winter, the project configured the rover for the winter environment. The project used the last drive opportunities to try to improve the northerly tilt of the rover. Unfortunately, this was unsuccessful and had little impact on the rover's already unfavorable tilt, with the arrays tilting south instead of north.

The unfavorable tilt of the rover made it susceptible to an increased risk of a low-power fault during the winter and further risk of a mission clock fault if the rover's batteries were depleted sufficiently. And of course, there was the risk of a complete loss of the rover from the harsh environment.

The project implemented a long-range set of DSN X-band and UHF communication passes to carry Spirit through the winter season. Communication windows were scheduled nine months into the future. The UHF passes in particular were complicated by orbit drift of the relay orbiters so far into the future. Spirit's fault windows were similarly complicated by clock drift over time. The project also updated some onboard fault protection parameters.

9 Loss of Signal, Probable Faults, and Recovery Effort

The last signal from Spirit occurred on Sol 2210 (2010-03-22). The first occurrence of loss of signal was on Sol 2218 (2010-03-30). Subsequent to the loss of signal, the project began the recovery effort for Spirit. That effort began with listening for the X-band fault windows (from low-power/Uploss fault) and for the autonomous UHF windows (from Uploss fault). As the continued lack of response suggested a possible mission clock fault, the project implemented a "Sweep&Beep" command strategy to elicit a response from the rover in the event the rover lost its knowledge of time.

All combinations of X-band and UHF transmit and receive hardware configurations were attempted as part of the recovery, along with commanding over a range of frequencies and times of day. Hardware (low-level) commands were attempted to exercise different boot banks within EEPROM. Between 2010-07-27 and 2011-07-13, 1411 commands were radiated as part of the recovery effort with no detection of any signal at X-band (both polarizations) or UHF (through the Mars orbiters).

The proximate cause for loss of the rover is not known, but is likely one of the following: (1) failure of a critical hardware element, such as the telecommunications (X-band and UHF) subsystem, the central computer systems or communications bus, the power subsystem (batteries, control board, switches), and the cabling; (2) insufficient energy from the solar arrays and batteries to permit rover wakeup; or (3) the complete mis-synchronization of the recovery commands with Mission Clock Fault.

The contributing causes include: (1) excessive dust on the rover solar arrays, reducing energy production; (2) the embedding at Troy, preventing favorable positioning of the solar arrays for winter; and (3) the fact that Spirit was well beyond design life with hardware that experienced thousands of deep thermal cycles. The ultimate root cause was likely the damaging effects of a very cold winter environment.

10 Lessons Learned

The MER Project made several changes to rover driving practices subsequent to the Spirit embedding at Troy. The project also implemented important changes to driving practices prior to Troy as a result of embedding events around the north and northeast parts of Home Plate, although these changes did not prevent the Troy embedding. The project now routinely produces Hazard Maps for drive planning in challenging or uncertain terrain. Further, the project established the Science Advisor role in tactical operations for mobility assessment. After Spirit's embedding at Troy, the project further implemented the 90% Slip Rule, where any detected occurrence of greater than 90% slip requires the project manager be notified and then requires project manager approval to resume driving. The project also advanced the analytic tools for mobility assessment with the development of sophisticated terra-mechanics modeling to investigate mobility-terrain interactions.

The project also made changes to fault protection parameters (on Opportunity) to enable better predictability in the event of fault conditions. The UP_TOO_LONG parameter was lengthened to avoid rover shut-downs before fault communication windows. The project disabled the coaxial switch change under the UPLOSS fault. This further avoids a potential switch failure on Opportunity.

An extensive repository of project lessons learned can be found in the MER project archive, Docushare Collection #23581.

11 Conclusion

Spirit landed in Gusev crater on January 4, 2004, then crossed the Gusev plains, climbed the Columbia Hills, reached the summit of Husband Hill, and then descended to Home Plate. The rover survived three Martian winters and two major dust storms. Last contact from Spirit was on March 22, 2010. Spirit's scientific discoveries include evidence of ancient water and carbonate minerals indicating neutral pH environments, the existence of ancient hydro-thermal systems, and probable recent (last obliquity change) water action on Mars.

By any measure, Spirit was a tremendous scientific and engineering success. The rover operated for 2210 sols and drove more than 7.7 kilometers, well beyond the original 90-sol duration and 1-kilometer distance requirements. The appendix contains a summary of accumulated rover parameters.

Acknowledgement: *This work was performed by the Jet Propulsion Laboratory, California Institute of Technology, under contract with the National Aeronautics and Space Administration.*

Appendix A—MER-A Trends (Sols 1 – 2210)

MER-A Actuator Use (Sols 1 – 2210)

Mobility Actuator	Motor Revs (M)
Left Front Wheel	18.747
Left Middle Wheel	17.450
Left Rear Wheel	17.953
Right Front Wheel	14.620
Right Middle Wheel	17.755
Right Rear Wheel	17.413
Left Front Steering	1.182
Left Rear Steering	1.248
Right Front Steering	1.109
Right Rear Steering	1.303

MER-A Notes:

Right front wheel failed on Sol 779

Right Rear Drive failed on Sols 2100–2101

Mobility Actuators tested lifetime: 10 million revs

Projected prime mission use: 2.5 million revs

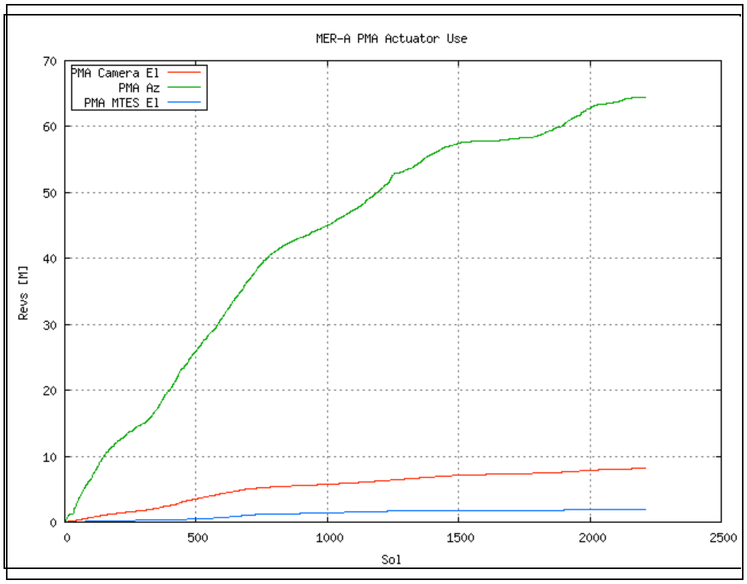

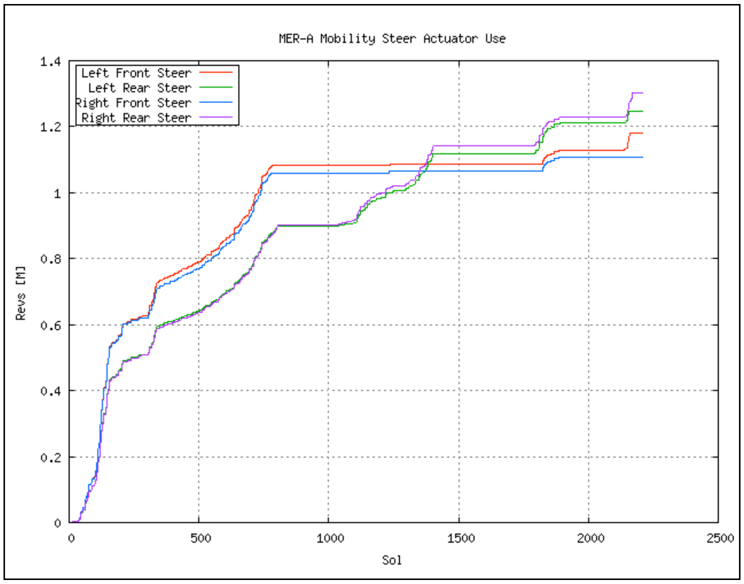

HGA Actuator	Motor Revs (M)
HGA Azimuth	4.083
HGA Elevation	5.590

MI Dust Cover Actuations	Actuations
MI Dust Cover	942

Note: *Each open is one actuation. Each close is one actuation.*

PMA Actuator	Motor Revs (M)

PMA Azimuth	64.440
PMA Camera Elevation	8.132
PMA MTES Mirror Elevation	1.899

IDD Actuator	Motor Revs (M)
IDD Shoulder Azimuth	1.824
IDD Shoulder Elevation	2.281
IDD Elbow	2.583
IDD Wrist	0.570
IDD Turret	1.397

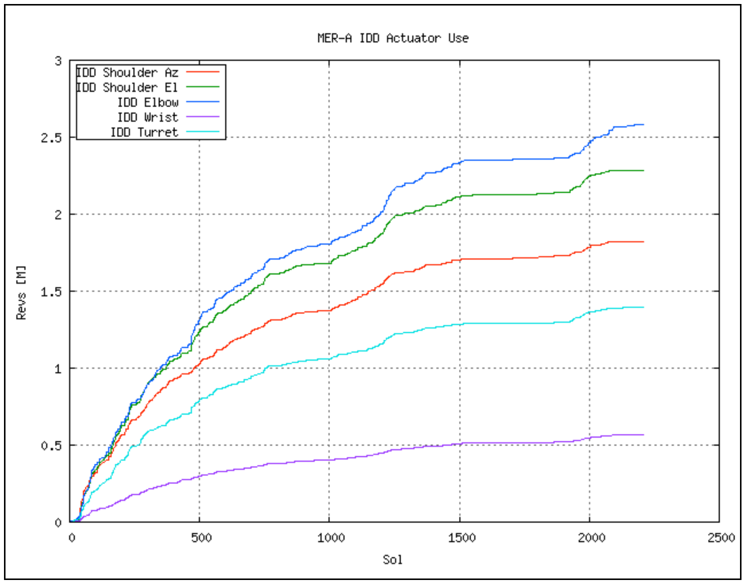

RAT Actuator	Motor Revs (M)
RAT Revolve	1.785
RAT Grind	16.284
RAT Actuator	**Distance (Meters)**
RAT Z	3.667

Note: *Encoder failures on RAT prevents accurate rev count.*
MER-A Note: *RAT grinding bit worn out*
MER-A Note: *RAT grind encoders failed on Sol 1341*

PMA Filter Wheel Actuator	Motor Revs (K)

PMA Left Filter Wheel	13.171
PMA Right Filter Wheel	11.526

MER-A Drive Data (Sols 1 – 2210)

Drive Parameters	Distance (Meters)
Drive Distance	7730.50

MER-A 3 Longest Drives (Sols 1 – 2210)

Distance	Sol
122.7	125
113.1	133
109.5	134

Drive Parameters	Number
Bumps to Position	177
Drives for Distance	302
Total Number of Drive Sols	479

Note: *Bumps indicate a drive with odometry less than 5 meters*

MER-A IDD Data (Sols 1 – 2210)

IDD Parameters	Number
IDD Sols	591

Note: *Number of IDD Sols is incremented each sol there is ANY movement in the IDD Joints*

MTES Use (Sols)	Number
MTES Sols	1546

IDD Tool Use (Sols)S	Number
MB	462
APXS	359
MI	356
RAT	101

Note: *Data in this table originates from*

MER-A Switch Use (Sols 1 – 2210)

Power Switches	Channel	Actuations
Camera Power Converter	P-0405	14376
Mobility Actuators Power	P-0513	7200
IDD Actuators Power	P-0515	2338
PMA Actuators Power	P-0517	58626
VME Power Converters Power	P-0506	0
Motor Control Board Logic Power Converters Power	P-0408	11058
IMU Power Converters Power	P-0482	2992
MB Power	P-0412	952
APXS Power	P-0413	730
RAT Power	P-0516	402
MTES Power	P-0454	8266
SDST Power	P-0467	656
SSPA A Power	P-0507	3355
SSPA B Power	P-0511	0
UHF Power	P-0512	5193
HGA Actuators Power	P-0518	2230
MI Heater Power	P-0401	20
RAT Heater Power	P-0464	2
MTES Heater A Power	P-0503	7
MTES Heater B Power	P-0487	7
REM Survival Heater A1 Power	P-0406	79
REM Survival Heater B1 Power	P-0402	79
REM Survival Heater A2 Power	P-0474	79
REM Survival Heater B2 Power	P-0466	79
Front HazCam Heaters Power	P-0468	38
Rear HazCam Heaters Power	P-0470	4
NavCam Heaters Power	P-0472	268
PanCam Warmup Heaters Power	P-0476	550
HGA Bearing Heaters Power	P-0489	476
HGA Actuators Heaters Power	P-0490	478
PanCam Bearing Heaters Power	P-0491	382
MCB FPGA Heater Power	P-0455	0
Left Wheel Heaters Power	P-0481	672
Right Wheel Heaters Power	P-0485	644

Note: *Each open is one actuation. Each close is one actuation.*

Note: *UHF radio is the same model as ODY. ODY uses 10k cycles (20k actuations) as lifetime.*

Telecom Switch Actuations	Channel	Actuations
WTS	T-0200	4313
Coax 0	T-0201	0
Coax 1	T-0202	43
Coax 2	T-0203	2

Note: *Each open is one actuation. Each close is one actuation.*
Note: *Waveguide switch and Coax switches rated at 10k cycles (20k actuations).*

MER-A Data Return (Sols 1 – 2210)

Data Return	GB	%
MGS	0.35	1.6
ODY	20.72	96.1
MRO	0.12	0.5
DTE	0.37	1.7
MEX	0.01	0.1
TOTAL DATA RETURN	**21.57**	

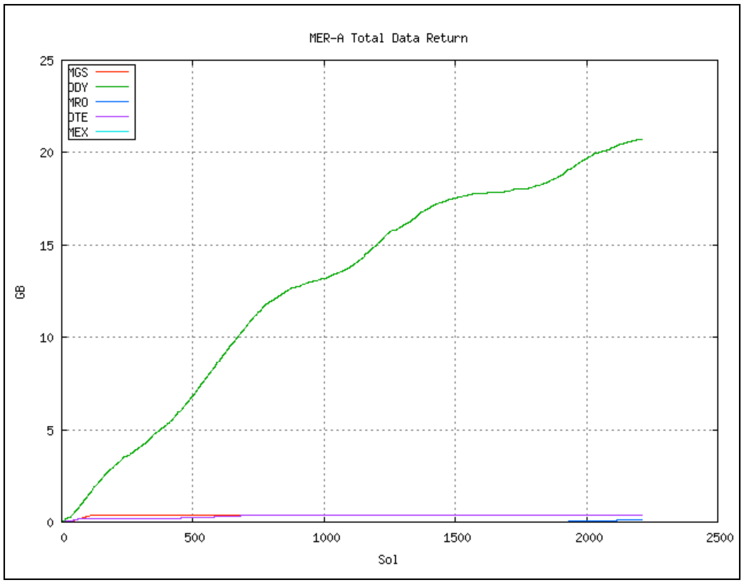

Average Data Return	Mb
Avg per Sol	79.96

MER-A Data Type (By APID) (Sols 1 – 2210)

Type	Volume (MB)	%
Real Time EHA	85.70	0.4
Real Time Info EVRs	2.39	0.0
Real Time Activity EVRs	7.83	0.0
Real Time Command EVRs	1.70	0.0
Real Time Warning EVRs	1.28	0.0
Left Pancam	5541.60	25.2
Right Pancam	4111.62	18.7
Left Navcam	2487.36	11.3
Right Navcam	1700.24	7.7
Left Front Hazcam	521.16	2.4
Right Front Hazcam	553.91	2.5
Left Rear Hazcam	280.28	1.3
Right Rear Hazcam	274.14	1.2
MI	1964.12	8.9
DI	1.31	0.0
MiniTES	2099.74	9.5
APXS	14.48	0.1
MB	111.12	0.5
RAT	32.80	0.1
IDD	62.37	0.3
Recorded EHA	422.81	1.9
Recorded Activity EVRs	67.51	0.3
Recorded Command EVRs	70.15	0.3
Recorded Warning EVRs	12.25	0.1
Recorded Fault EVRs	0.05	0.0
Comm Engineering	60.12	0.3
HGA and PMA	323.88	1.5
EDL Recorded	2.49	0.0
FSW Engineering	642.80	2.9
ACS Engineering	0.04	0.0
Motor Control	30.65	0.1
Mobility Engineering	517.79	2.4

MER-A Data Return Summary (Sols 1 – 2210)

Type	Volume (GB)	%
Engineering Channelized	0.50	2.3
Engineering EVRs	0.16	0.7
Engineering Images	5.68	26.4
Engineering DPs	1.60	7.5
Science Images	11.35	52.8
Science DPs	2.21	10.3
Total Data Returned	21.57	100

MER-A Warning EVR Summary (Sols 1 – 2210)

Warning EVR Type	Total Count
Single Event Upsets	23
Remote Engineering Unit Invalid Response	38
Acquisition Error Warnings	21
Write Verification Error	0
Interface Electronics to Stepper Motor	10

MER-A Misc Data (Sols 1 – 2210)

Radiation Source	Type	Strength At Landing	Current Strength	% Remaining
Mossbauer Source	Cobalt 57 (gamma ray)	150 mCi	0.46 mCi	0.3
APXS Source	Curium 244 (alpha particle & X-ray)	30 mCi	23.64 mCi	78.8
RHU Source*	Plutonium 238 (alpha particle)	33.6 Ci / 1 Watt	31.99 Ci/ 0.95 Watts	95.2

**RHU Strength was 1 Watt at delivery, not 1 Watt at landing.*

MER-A Summary of Image Source Totals, Sol 1 to Sol 2210

Source Images	Total Counts
EDL Images	3
Front Hazcam Images	7,432
Rear Hazcam Images	3,351
MI Images	6,053
Navcam Images	27,432
Pancam Images	80,568
TOTAL NUMBER OF MER-A IMAGES	**124,839**

Appendix B—Acronym List

AEGIS	Autonomous Exploration for Gathering Increased Science
APAM	Activity Plan Approval Meeting
APXS	Alpha Particle X-ray Spectrometer
DSN	Deep Space Network
EDR	Experimental Data Record
ECAM	Engineering Camera
ERT	Earth Receive Time
FSW	Flight Software
GDS	Ground Data System
Hazcam	Hazard Avoidance Camera
HGA	High-gain Antenna
IDD	Instrument Deployment Device
IST	Integrated Sequence Team
IVP	Inertial Vector Propagator
JPL	Jet Propulsion Laboratory
KOP	Keeper of the Plan
LGA	Low-gain Antenna
MB	Moessbauer Spectrometer
MCT	Mission Control Team
MDOT	Mission Data Operations Team
MER	Mars Exploration Rover
MI	Microscopic Imager
MIPL	Multi-mission Image Process Lab (Team)
MM	Mission Manager
Mini-TES	Miniature Thermal Emission Spectrometer
MRO	Mars Reconnaissance Orbiter
MSL	Mars Science Laboratory
NAIF	Navigation and Ancillary Information Facility
NASA	National Aeronautics and Space Administration
Navcam	Navigation Camera
ODY	Mars Odyssey
OSS	Operations Storage Server
Pancam	Panoramic Camera
PDL	Payload Downlink Lead
PDS	Planetary Data System
PMA	Pancam Mast Assembly
PUL	Payload Uplink Lead
RAT	Rock Abrasion Tool
RDR	Reduced Data Record
REM	Rover Electronics Module
SOST	Science Operations Support Team
SOWG	Science Operations Working Group
SRET	Spacecraft/Rover Engineering Team
SSTB	Surface System Testbed
TAP/SIE	Tactical Activity Planner/Sequence Integration Engineer
TDL	Tactical Downlink Lead
TUL	Tactical Uplink Lead
UHF	Ultra High Frequency
UTC	Universal Time Coordinated
WEB	Warm Electronics Box